Tail risk in government bond markets and ECB unconventional policies*

Xin Zhang,[(a)] *Bernd Schwaab*[(b)]

[(a)] Sveriges Riksbank, Research Division

[(b)] European Central Bank, Financial Research

March 7, 2016

Abstract

This paper derives a novel observation-driven model to study the time variation in the tail shape for time series observations from a wide class of fat-tailed distributions. Monte Carlo experiments suggest that the model reliably captures tail shape variation in a variety of simulation settings. In an empirical study of sovereign bond yields at a high frequency, we demonstrate that unconventional monetary policies adopted by the European Central Bank between 2010–2012, specifically its Securities Markets Programme and Outright Monetary Transactions, lowered the tail risk associated with holding certain sovereign bonds during the euro area sovereign debt crisis.

Keywords: tail risk, observation-driven models, extreme value theory, European Central Bank (ECB), Securities Markets Programme (SMP).

JEL classification: *C22, G11.*

*Author information: Xin Zhang, Research Division, Sveriges Riksbank, SE 103 37 Stockholm, Sweden, email: xin.zhang@riksbank.se. Bernd Schwaab, Financial Research, European Central Bank, Sonnemannstrasse 22, 60314 Frankfurt, Germany, email: bernd.schwaab@ecb.int. We thank Simone Manganelli, Daniele Massacci, and David Veredas for comments, as well as seminar participants at the Sveriges Riksbank and European Central Bank. The views expressed in this paper are those of the author and they do not necessarily reflect the views or policies of the Sveriges Riksbank or European Central Bank.

1 Introduction

We propose a novel observation-driven model that introduces time series dynamics into the tail shape parameter of the Generalized Pareto Distribution (GPD). The GPD is of considerable interest to financial economists, as it is the only non-degenerate density that approximates the distribution of data exceedances beyond a given threshold; see, for example, Davidson and Smith (1990), Embrechts, Klüppelberg, and Mikosch (1997), and McNeil, Frey, and Embrechts (2010, Chapter 7). As a result, it plays a central role in the study of extremes, comparable to the role the normal distribution plays in the study of observations with finite variance. The proposed framework allows us to track the time variation in the tail index of observations from a wide class of fat-tailed distributions; see Rocco (2014) for a recent survey of extreme value theory (EVT) methods.

In our model, the tail shape dynamics are driven by the score of the predictive log-likelihood. So-called Generalized Autoregressive Score (GAS) models were developed in their full generality in Creal, Koopman, and Lucas (2013); see also Harvey (2013) for a textbook treatment. In this setting, the time-varying parameter is perfectly predictable one step ahead. This feature makes the new model observation-driven; see Cox (1981). The likelihood is known in closed-form through a standard prediction error decomposition, making parameter estimation straightforward via maximum likelihood procedures.

Extensive Monte Carlo experiments suggest that our score-driven model reliably captures tail shape variation in a variety of simulation settings. In addition, the treatment of non-tail observations is an important concern in the dynamic modeling of the tail shape parameter. We therefore consider different approaches to the treatment of such observations in each simulation: deletion, modeling as missing without information on the tail, and as a draw from a mixture density with a point mass at zero. We find that the simple deletion of missing values is appropriate if a complete time series of tail shape estimates is not required, and tail fatness is sufficiently high. Modeling non-tail observations as missing works well if mean reversion in the time-varying tail shape parameter is strong, regardless of the fatness in the tail. Modeling the tail shape dynamics based on a mixture distribution performs well when

mean reversion is less pronounced, and the tail is not as fat.

We apply our score-driven modeling framework to study sovereign bond yields at a high frequency for five euro area countries: Greece, Ireland, Italy, Portugal, and Spain. We demonstrate that two unconventional monetary policy measures involving asset purchases adopted by the European Central Bank during the euro area sovereign debt crisis, specifically its Securities Markets Programme (SMP) and the Outright Monetary Transactions (OMT) program, helped lower the fatness of the right (bad) tail as well as the market risk associated with holding certain sovereign bonds between 2010–2012. This is relevant since elevated tail risks alone can force institutional investors and market makers to retreat from a given market, particularly if value-at-risk constraints are binding; see, for example, Vayanos and Vila (2009), and Adrian and Shin (2010). For anecdotal evidence that market makers withdrew from trading Italian debt securities in 2011, see Pelizzon, Subrahmanyam, Tomio, and Uno (2013).

For government bond purchases undertaken within the SMP, we disentangle announcement effects from the impact owing to the implementation of announced purchases, and find that announcement effects are more important. For example, we estimate that the announcement of the SMP on 10 May 2010 reduced the 15-minute Expected Shortfall associated with holding five-year government bonds by approximately -1.1 basis points (bps, Portugal), -1.5 bps (Spain), -2.2 bps (Italy), -3.5 bps (Ireland), and up to -5.4 bps (Greece). These reductions are economically meaningful given the prevailing market risks at that time, and the fact that the impact of asset purchases as considered in this paper are in addition to the effects on the conditional mean and variance of bond yields as documented in Ghysels, Idier, Manganelli, and Vergote (2016), and Eser and Schwaab (2016). The immediate market risk impact of the OMT announcement on 06 September 2012 ranges between approximately zero (Italy) and -2 bps (Ireland), from lower levels of market risk at the time. As a result, the announcement of unconventional monetary policies likely contributed towards restoring depth and liquidity in impaired markets by allowing market makers to remain active during turbulent times. By contrast, we find that the implementation of announced purchases did not have an economically meaningful effect on tail risk in a setting where variation in the

conditional variance is controlled for.

Based on our dynamic EVT framework, we also find that euro area government bonds differed substantially in terms of tail shape and market risk during the euro area sovereign debt crisis. Italian and Spanish bonds had the lowest (among the five SMP countries) estimated 15-minute 99% Expected Shortfall, of up to approximately 50 bps. By contrast, Greek bonds had a high estimated Expected Shortfall, of up to approximately 300 bps, particularly in the months leading up to the credit event on 09 March 2012. These are extreme levels of market risk. Interestingly, different market segments also experienced peak market stress at different times. The highest tail risks are observed relatively late in Spain and Italy, with pronounced peaks in 2011Q4. By contrast, elevated market stress materialized already much earlier for Greek, Irish and Portuguese bonds, between 2010 – 2011. This is approximately in line with standard accounts of the debt crisis; see, for example, Eser et al. (2012), and Cœuré (2013), according to which smaller countries in the periphery of the euro area were affected first, and larger countries such as Italy and Spain were affected later.

Several studies investigate the dynamic behavior of the tail index. Quintos, Fan, and Phillips (2001) derive formal tests for time-variation in the tail index. A number of subsequent studies apply these tests to financial time series data. For example, Werner and Upper (2004) identify several breaks in the tail behavior of high-frequency German Bund future returns. Similarly, Galbraith and Zernov (2004) demonstrate that certain regulatory changes in U.S. equity markets altered the tail index dynamics of equities returns, while Wagner (2005) argues that changes in government bond yields exhibit time-variation in the tail shape for both the U.S. and the euro area. Another promising strand of the EVT literature exploits the high-dimensional panel structure of many datasets. For example, Kelly (2014) develops a power law model for cross-sectional tail risk that takes a GARCH-type autoregressive form. Building on this framework, Kelly and Jiang (2014) link the common fluctuations in equity tail risk to other asset returns and macro-economic aggregates. Finally, (dynamic) EVT has been applied in the study of systemic risk; see Hartmann, Straetmans, and de Vries (2004, 2007), and Allen, Bali, and Tang (2012).

The methodological part of this paper is closest to Massacci (2014). Massacci proposes an observation-driven time series model for both the tail and scale parameters in the GPD distribution of a univariate time series. Both parameters evolve in a bivariate system, and are updated jointly based on the scaled score of the tail shape parameter. This approach is an important addition to the dynamic EVT literature. However, it takes the view that researchers are unwilling to work with pre-filtered data in practise. This is not always the case; see McNeil and Frey (2000), Poon, Rockinger, and Tawn (2004), Brownlees and Engle (2015), Lucas, Schwaab, and Zhang (2014, 2016), and others. If the data are de-volatized based on an appropriate volatility model in a first step, the scale of the GPD becomes fixed (at unity), leaving only one time-varying parameter to model. Our framework is different in that our approach allows for more flexibility in the joint modeling of scale and the tail shape parameter. In addition, we explore when the modeling of tail shape based on a mixture distribution may not work as well as other approaches, and provide expressions for the score and scaling function for these alternatives as well.

We proceed as follows. Section 2 introduces the statistical model. Section 3 provides evidence from an extensive Monte Carlo study. Section 4 applies the model to euro area sovereign bond yields. Section 5 concludes.

2 Statistical model

2.1 Time-varying tail risk

This section introduces time variation into the tail shape parameter $\xi_t > 0$ of the Generalized Pareto Distribution (GPD). The probability density function (pdf) of a GPD distributed random variable $x_t > 0$ is given by

$$p(x_t; \delta, \xi_t) = \frac{1}{\delta}\left(1 + \xi_t \frac{x_t}{\delta}\right)^{-\frac{1}{\xi_t}-1}, \tag{1}$$

where $x_t = y_t - \tau > 0$ is the so-called peak-over-threshold (POT), or exceedance, of fat-tailed data y_t over a pre-determined threshold τ, $\delta > 0$ is an additional scale (variance)

parameter, and $\xi_t > 0$ is the tail shape parameter; see, for example, McNeil, Frey, and Embrechts (2010).[1] If $y_t - \tau \leq 0$, we may consider x_t as missing, or as a draw from a mixture distribution, see Section 2.2 below. As a result, exceedances $x = (x_1, \ldots, x_T)$ and data $y = (y_1, \ldots, y_T)$, $t = 1, \ldots, T$, are univariate time series at the same frequency. The cumulative distribution function (cdf) and the log-likelihood of x_t is given by

$$P(x_t; \delta, \xi_t) = 1 - \left(1 + \xi_t \frac{x_t}{\delta}\right)^{-\frac{1}{\xi_t}}, \qquad l(x_t; \delta, \xi_t) = -\ln(\delta) - \left(1 + \frac{1}{\xi_t}\right) \ln\left(1 + \xi_t \frac{x_t}{\delta}\right), \quad (2)$$

respectively.

We assume that the pdf of y_t, $g(y_t)$, is a fat-tailed distribution with time-varying tail index $\alpha_t > 0$, such as, for example, a univariate Student's t distribution with $\nu_t = \alpha_t = 1/\xi_t$ degrees of freedom. In this case the cumulative distribution function $G(y_t)$ can be expressed as $G(y_t) = G(\tau) + (1 - G(\tau))P(x_t)$ for sufficiently high values of τ. As a result, all interesting tail behavior is captured by $p(x_t; \delta, \xi_t)$.[2]

Following Creal, Koopman, and Lucas (2013), and Harvey (2013), we endow ξ_t with score-driven (GAS) dynamics using the derivative of the log conditional observation density (1). We ensure positive values of ξ_t by specifying $\xi_t = \exp(f_t)$. The transition dynamics for f_t are given by

$$f_{t+1} = \omega + \sum_{i=0}^{p-1} a_i s_{t-i} + \sum_{j=0}^{q-1} b_j f_{t-j}, \quad (3)$$

$$s_t = \mathcal{S}_t \nabla_t, \quad \nabla_t = \partial \ln p(x_t | \mathcal{F}_{t-1}; f_t, \psi) / \partial f_t,$$

where $\omega = \omega(\psi)$ is a fixed intercept, $a_i = a_i(\psi)$ and $b_j = b_j(\psi)$ are fixed scalar parameters

[1] Essentially all common continuous distributions of statistics and the actuarial sciences lie in a certain Maximum Domain of Attraction (MDA); see McNeil et al. (2010, Chapter 7.1). When considering $\xi_t > 0 \, \forall \, t$ we implicitly assume that a Fréchet limit (a power tail) applies. Examples of such distributions are Student's t, inverse gamma, loggamma, F, Fréchet, and Burr.

[2] The choice of threshold τ is subject to a well-known bias-efficiency tradeoff; see, for instance, McNeil and Frey (2000). In theory, the limit distribution of exceedances holds exactly only as the threshold $\tau \to +\infty$. A higher threshold, however, also implies a smaller number of exceedances, and consequently an increased sampling error in the estimation of the tail shape parameter. We address this issue by considering multiple choices for τ in our empirical application. The 10% and 5% empirical quantile are common choices in the literature; see Chavez-Demoulin, Embrechts, and Sardy (2014).

that depend on the vector ψ containing all time invariant parameters in the model, and $\mathcal{F}_{t-1} = \{x_1, \ldots, x_{t-1}\}$.

For the remainder of the paper, we make three empirical choices. First, we select the inverse conditional Fisher information of the observation density as our scaling function, $\mathcal{S}_t = \mathrm{E}[\nabla_t^2 | \mathcal{F}_{t-1}; f_t, \psi]^{-1} = \mathrm{E}[-\partial \nabla_t(x_t|\mathcal{F}_{t-1}; f_t, \psi)/\partial f_t]^{-1}$. Creal, Koopman, and Lucas (2013) and Creal, Schwaab, Koopman, and Lucas (2014) demonstrate that this choice of scaling function results in a stable model, and effectively yields a Gauss-Newton update of f_t over time. Second, we consider a fixed $\delta = 1$ throughout the paper. This corresponds to the common practise of using volatility-filtered data before considering tail risk dynamics. If volatility clustering is not accounted for, movements in the tail may be confounded with movements in the conditional variance; see, for example, McNeil and Frey (2000). Finally, we assume $p = q = 1$ in (3), such that $a = a_0$ and $b = b_0$. Higher order terms are rarely necessary in practise; see Creal et al. (2013). To ensure stationarity of the factor process we require $\mid b \mid < 1$, and in addition restrict $a > 0$.

2.2 Treatment of non-tail observations

This section discusses three different approaches to the handling of non-tail observations $y_t \leq \tau$, and provides the resulting expressions for the conditional score ∇_t and scaling function $\mathcal{S}_t$ in (3). We consider the performance of these three approaches in our simulation experiments in Section 3.

First, we simply decide to delete the missing entries in the univariate time series. This yields a substantially shorter time series for x. In this case, closed-form expressions for the score s_t and the scaling function $\mathcal{S}_t$ can be derived as

$$\nabla_t = \frac{1}{\xi_t} \ln\left(1 + \xi_t \frac{x_t}{\delta}\right) - (\xi_t + 1)\frac{x_t}{\delta + \xi_t x_t}, \tag{4}$$

$$\mathcal{S}_t = \frac{(1 + 2\xi_t)(1 + \xi_t)}{2\xi_t^2}, \tag{5}$$

where, again, $\mathcal{S}_t = \mathrm{E}[-\partial \nabla_t(x_t|\mathcal{F}_{t-1}; f_t, \psi)/\partial f_t]^{-1}$ is the inverse conditional Fisher information quantity for x_t. We refer to Appendix A1 for the derivation of (4) – (5). Deleting non-tail

observations before applying (1) – (5) is straightforward, and in line with the spirit of EVT in the absence of time variation in the tail index; see McNeil, Frey, and Embrechts (2010, Chapter 7). One immediate downside of this approach, however, is that ξ_t is unavailable for all $y_t \leq \tau$.

Second, we calculate the scaled score (4) – (5) only if x_t is observed, and assign a zero value to the scaled score if x_t is missing. This approach is adopted in Creal, Schwaab, Koopman, and Lucas (2014). The updating equation becomes

$$f_{t+1} = \omega + a \cdot \mathrm{I}(x_t > 0)\mathcal{S}_t \nabla_t + b \cdot f_t. \tag{6}$$

As a result, $f_t = \ln(\xi_t)$ slowly reverts back to its unconditional mean $\omega/(1-b)$ in the absence of new information from the tail. The updating equation (6) takes into account that ξ_t evolves as a continuous process which governs the tail behavior of each y_t. An estimate of ξ_t is now available at any time t.

Finally, we use a mixture distribution to model the exceedance and to derive the score; see, for example, Davidson and Smith (1990), and Massacci (2014). In this case, observations $y_t \leq \tau$ generate the POT values $x_t = 0$. This approach allows us to incorporate information in the tail as well as from the center of the distribution. We consider the mixture

$$\phi(x_t; \delta, \xi_t) = \mathrm{I}(x_t > 0)\left[(1+\tau)^{-\frac{1}{\xi_t}}\frac{1}{\delta}\left(1+\xi_t\frac{x_t}{\delta}\right)^{-\frac{1}{\xi_t}-1}\right] + \mathrm{I}(x_t = 0)\left(1-(1+\tau)^{-\frac{1}{\xi_t}}\right), \tag{7}$$

where the GPD pdf applies with tail probability $\bar{G}(\tau) = (1+\tau)^{-\frac{1}{\xi_t}}$.[3] The respective log-likelihood is

$$\begin{aligned} \ell(x_t; \delta, \xi_t) &= \mathrm{I}(x_t > 0)\left[-\frac{1}{\xi_t}\ln(1+\tau) - \ln(\delta) - \left(1+\frac{1}{\xi_t}\right)\ln\left(1+\xi_t\frac{x_t}{\delta}\right)\right] \\ &+ \mathrm{I}(x_t = 0)\ln(1-(1+\tau)^{-\frac{1}{\xi_t}}). \end{aligned} \tag{8}$$

[3]The tail probability is common across fat-tailed distributions $g(y_t)$. If $G(y_t)$ lies in the MDA of the Fréchet limit (see footnote 1, and McNeil, Frey, and Embrechts (2010, p. 268)), the survival function of y_t can be written as $\bar{G}(y_t) = y_t^{-1/\xi_t} \cdot L(y_t)$, where $L(y_t)$ is a slowly varying function. Adopting the choice $L(y_t) = (y_t/(1+y_t))^{1/\xi_t}$ yields the tail probability below (7).

The score-driven update of $f_t = \ln \xi_t$ becomes slightly more involved in this case. The score and scaling function are now given by

$$\begin{aligned} \nabla_t &= \mathrm{I}(x_t > 0) \left[\frac{1}{\xi_t} \ln(1+\tau) + \frac{1}{\xi_t} \ln\left(1 + \xi_t \frac{x_t}{\delta}\right) - (\xi_t + 1) \frac{x_t}{\delta + \xi_t x_t} \right] \\ &- \mathrm{I}(x_t = 0) \left[\frac{(1+\tau)^{-\frac{1}{\xi_t}}}{1 - (1+\tau)^{-\frac{1}{\xi_t}}} \frac{1}{\xi_t} \ln(1+\tau) \right], \end{aligned} \tag{9}$$

and

$$\mathcal{S}_t = \left[\frac{2\xi_t^2 (1+\tau)^{-\frac{1}{\xi_t}}}{(1+2\xi_t)(1+\xi_t)} + \frac{(1+\tau)^{-\frac{1}{\xi_t}}}{1 - (1+\tau)^{-\frac{1}{\xi_t}}} \frac{1}{\xi_t^2} \ln(1+\tau)^2 \right]^{-1}, \tag{10}$$

respectively. We refer to Appendix A2 for the derivation of (9)–(10). Since both expressions are available in closed form, the transition equation for f_t is straightforward.[4] Modeling the tail index as the inverse tail shape $\alpha_t = 1/\xi_t$ in a score-driven way leads to equivalent expressions for the score and the same scaling function.

2.3 Explanatory covariates

This section extends the score-driven mechanism for the time-varying tail shape to include lagged values of economic variables as additional conditioning variables. For example, ECB asset purchases may help explain the time variation in the right tail shape. As an extension, we consider score-driven dynamics (9) – (10) with factor dynamics that include ECB asset purchases,

$$f_{t+1} = \omega + a \cdot s_t + b \cdot f_t + c \cdot \mathrm{SMP}_t + d \cdot \mathrm{SMP}_{t-1}, \tag{11}$$

where the additional right-hand side variables SMP_t are daily purchase volumes in €billion of par value. Time differences in purchase volumes, or dummy variables indicating purchases, are alternative conditioning variables. Intraday values are held constant at the daily levels. We consider the extended specification (11) in Section 4.2.

[4] Computer code will be made available on `http://www.gasmodel.com`.

3 Simulation study

This section presents our Monte Carlo simulation results. We are particularly interested in two questions: whether our statistical framework reliably recovers time variation in the tail shape, and which treatment of non-tail observations is appropriate.

We chose the Student's t distribution $y_t \sim \text{t}(\nu)$ as our fat tailed distribution $g(y_t)$, and consider three values for the degrees of freedom parameter, $\nu = 3, 5, 7$. The threshold τ is the 90% percentile of the random sample generated from a $t(3)$ and $t(5)$ distribution, and the 95% percentile when the sample is generated from the $t(7)$ distribution (for which the tail is less fat). The exceedance sample contains $x_t \sim \text{GPD}(0, \delta, \xi_t)$ if $y_t > \tau$, and zero (missing) otherwise. The GPD distributed random variables are drawn as $x_t = \delta \frac{u_t^{-\xi_t} - 1}{\xi_t}$, where $u_t \sim \text{U}[0, 1]$ is uniform.

Each simulation uses a different path for the tail shape parameter $\xi_t = \exp(f_t)$. We consider seven data generating processes (DGP). The first four processes are stylized dynamics in the literature; see, for example, Lucas and Zhang (2016). The final three processes consider random draws of f_t subject to different parameters ψ.

(1) Constant: $\xi_t = 0.9$,

(2) Sine: $\xi_t = 0.5 + 0.4\cos(2\pi t/200)$,

(3) Fast Sine: $\xi_t = 0.5 + 0.4\cos(2\pi t/20)$,

(4) Step: $\xi_t = 0.9 - 0.5(t > 500)$,

(5) sGPD^d : (delete missings) $f_{t+1} = \omega + a\mathcal{S}_t\nabla_t + bf_t$,

(6) sGPD^z : (assign zero) $f_{t+1} = \omega + a \cdot \text{I}(x_t > 0)\mathcal{S}_t\nabla_t + bf_t$,

(7) sGPD^m : (mixture density): $f_{t+1} = \omega + a\mathcal{S}_t\nabla_t + bf_t$,

The parameters in simulation settings (5) – (7) are chosen in two different ways, as

$$\begin{aligned} \psi_1 \quad &: \quad \omega = -0.025, a = 0.01, b = 0.97, \delta = 1, \\ \text{and} \quad \psi_2 \quad &: \quad \omega = 0.01, a = 0.12, b = 0.85, \delta = 1. \end{aligned}$$

As a result, the tail risk dynamics under parameter vector ψ_1 are more persistent than in the

model with ψ_2; note the higher value for b. In addition to exhibiting faster mean reversion, the tails are also fatter under ψ_2, as the unconditional mean of f_t is higher.

We end up with $4+2\times 3 = 10$ stochastic GPDs, in three environments ($\nu = 3, 5, 7$). This yields 30 data generating processes. For each DGP, we draw 100 simulation samples of y with $10,000$ observations each. As a result, approximately 1,000 ($t(\nu = 3, 5)$) or 500 ($t(\nu = 7)$) tail observations are used to construct POT values. Our main metric for evaluating model performance is Mean Absolute Error, MAE $= \frac{1}{ST}\sum_{s=1}^{S}\sum_{t=1}^{T}|\hat{\xi}_{st} - \xi_{st}|$, where $\hat{\xi}_{st}$ is the estimated dynamic tail parameter in simulation s, ξ_{st} is the true tail shape, S is the number of simulations, and T is the number of observations in each draw.

Table 1 presents the main MAE simulation outcomes. We focus on three main findings. First, simply deleting missing values (our first approach) seems to be permissible as long as the tail fatness is sufficiently high. When $\nu = 3$, the respective factor estimates are close to the underlying true processes in many cases. Even if the true tail dynamics come from a mixture-likelihood model, the sGPD^d and sGPD^z approaches still deliver close estimates. Modeling non-tail observations as missing, without information about the tail, works well if mean reversion in the tail shape process is strong (ψ_2), but not necessarily otherwise (ψ_1).

As the degrees of freedom parameter increases and the sample size decreases ($\nu = 7$), the appropriateness of simply deleting missing values in x becomes less clear. In all DGPs under ψ_1, the mixture model sGPD^m now outperforms the other approaches; see columns 6, 8, and 10. This is not surprising. When the tail observations are less frequent and contain less information about the (thinner) tail, then the mixture-density model benefits from being able to take into account information from non-tail observations as well. If the tails are fatter (ψ_2), the first two approaches are again appropriate.

Second, the standard deviations about the MAE statistics are typically larger in the first two rows than for the mixture-density approach. This difference in standard errors points towards a loss of efficiency that occurs when we discard observations (as in the first approach), or model them by a zero value for the score (the second approach). Again, the mixture-density approach uses non-tail observations to at least some degree, implying less variation across simulations for these estimates.

Table 1: **Simulation results: Mean Absolute Error**

The table reports mean absolute error (MAE) statistics for 10 DGPs (columns) and three estimation approaches (rows), in three environments (top, middle, and bottom panels). The hit variable $\mathrm{I}(y_t > \tau)$ is simulated from a $t(3)$, $t(5)$, and $t(7)$. We consider 100 simulations for each DGP, and a time series y of $10,000$ observations in each simulation. Different approaches to the treatment of non-tail observations are indicated in the respective rows. sGPD^d deletes missing vales, sGPD^z assigns a zero value to the score at missing values, and sGPD^m uses a mixture density. Model performance is measured by the MAE from the true ξ_t in each draw. The number in bold indicates minimum MAE among the four approaches considered. For DGPs (5)–(8), two sets of parameters ψ_1 and ψ_2 apply.

Model	(1)	(2)	(3)	(4)	(5)-ψ_1	(5)-ψ_2	(6)-ψ_1	(6)-ψ_2	(7)-ψ_1	(7)-ψ_2
					t distributed, $\nu = 3$					
sGPD^d	0.049	**0.202**	0.259	**0.151**	**0.045**	**0.097**	**0.038**	**0.100**	0.044	0.136
	(0.037)	(0.016)	(0.006)	(0.044)	(0.022)	(0.064)	(0.021)	(0.031)	(0.018)	(0.017)
sGPD^z	**0.046**	0.293	0.260	0.274	0.054	0.534	0.040	0.123	**0.043**	**0.136**
	(0.037)	(0.042)	(0.008)	(0.040)	(0.028)	(0.139)	(0.029)	(0.052)	(0.024)	(0.020)
sGPD^m	0.359	0.255	**0.255**	0.249	0.092	0.619	0.090	0.528	0.061	0.300
	(0.008)	(0.001)	(0.001)	(0.002)	(0.013)	(0.065)	(0.008)	(0.010)	(0.006)	(0.006)
					t distributed, $\nu = 5$					
sGPD^d	0.048	**0.201**	0.258	**0.152**	0.043	**0.082**	0.036	**0.101**	0.039	0.108
	(0.034)	(0.015)	(0.006)	(0.046)	(0.022)	(0.037)	(0.021)	(0.032)	(0.019)	(0.015)
sGPD^z	**0.045**	0.297	0.259	0.280	0.057	0.566	0.036	0.117	0.036	**0.106**
	(0.035)	(0.040)	(0.012)	(0.046)	(0.026)	(0.154)	(0.022)	(0.047)	(0.018)	(0.016)
sGPD^m	0.433	0.256	**0.257**	0.249	**0.041**	0.695	**0.021**	0.603	**0.019**	0.313
	(0.007)	(0.001)	(0.001)	(0.002)	(0.005)	(0.064)	(0.005)	(0.008)	(0.003)	(0.005)
					t distributed, $\nu = 7$					
sGPD^d	0.069	**0.209**	0.260	0.066	0.058	**0.142**	0.050	0.097	0.052	0.096
	(0.046)	(0.026)	(0.009)	(0.049)	(0.031)	(0.076)	(0.034)	(0.046)	(0.032)	(0.033)
sGPD^z	**0.062**	0.314	**0.259**	**0.059**	0.060	0.504	0.043	**0.088**	0.045	**0.090**
	(0.044)	(0.113)	(0.007)	(0.046)	(0.030)	(0.221)	(0.032)	(0.047)	(0.029)	(0.029)
sGPD^m	0.477	0.260	0.261	0.477	**0.039**	0.740	**0.022**	0.646	**0.020**	0.344
	(0.006)	(0.001)	(0.001)	(0.006)	(0.010)	(0.090)	(0.005)	(0.010)	(0.002)	(0.005)

Finally, the results are overall not too sensitive to which exact model is employed for inference on ξ_t. For example, the mixture density approach is accurate even if the true model is formulated differently. In other words, even (slightly) misspecified score-driven models appear to work well. Blasques, Koopman, and Lucas (2015) prove that score-based parameter updates always reduce the local Kullback-Leibler divergence between the true conditional density and the (potentially misspecified) model-implied conditional density, and are in this sense optimal from an information theoretic perspective. Table 1 suggests that slightly misspecified models can still work well in practise.

Table 2 presents the mean squared error outcomes, $\mathrm{MSE} = \frac{1}{ST}\sum_{s=1}^{S}\sum_{t=1}^{T}(\hat{\xi}_{st} - \xi_{st})^2$, where S and T are as defined above. The MSE statistics correspond to a quadratic loss

Table 2: **Simulation results: Mean Squared Error**

The table reports mean squared error (MSE) statistics for 10 DGPs (columns) and three estimation approaches (rows), in three environments (top, middle, and bottom panels). The hit variable $\mathrm{I}(y_t > \tau)$ is simulated from a $t(3)$, $t(5)$, and $t(7)$. We consider 100 simulations for each DGP, and a time series y of $10,000$ observations in each simulation. Different approaches to the treatment of non-tail observations are indicated in the respective rows. sGPD^d deletes missing vales, sGPD^z assigns a zero value to the score at missing values, and sGPD^m uses a mixture density. The number in bold indicates minimum MAE among the four approaches considered. For DGPs (5)–(8), two sets of parameters ψ_1 and ψ_2 apply.

Model	(1)	(2)	(3)	(4)	(5)-ψ_1	(5)-ψ_2	(6)-ψ_1	(6)-ψ_2	(7)-ψ_1	(7)-ψ_2
					t distributed, $\nu = 3$					
sGPD^d	0.004	**0.057**	0.086	**0.034**	**0.004**	**0.052**	**0.003**	**0.039**	0.004	0.033
	(0.006)	(0.010)	(0.007)	(0.015)	(0.004)	(0.085)	(0.004)	(0.027)	(0.003)	(0.008)
sGPD^z	**0.004**	0.127	0.086	0.124	0.005	0.933	0.004	0.119	**0.004**	**0.033**
	(0.005)	(0.053)	(0.009)	(0.319)	(0.007)	(1.039)	(0.010)	(0.340)	(0.007)	(0.010)
sGPD^m	0.129	0.081	**0.081**	0.076	0.010	0.882	0.008	0.315	0.004	0.117
	(0.006)	(0.001)	(0.001)	(0.002)	(0.002)	(0.613)	(0.002)	(0.027)	(0.001)	(0.006)
					t distributed, $\nu = 5$					
sGPD^d	0.004	**0.058**	0.085	**0.040**	0.003	**0.030**	0.002	**0.044**	0.003	0.019
	(0.005)	(0.011)	(0.009)	(0.052)	(0.003)	(0.035)	(0.003)	(0.058)	(0.003)	(0.005)
sGPD^z	**0.004**	0.131	0.088	0.104	0.006	0.961	0.002	0.060	0.002	**0.018**
	(0.005)	(0.051)	(0.040)	(0.062)	(0.006)	(0.720)	(0.003)	(0.074)	(0.002)	(0.004)
sGPD^m	0.187	0.082	**0.082**	0.099	**0.003**	0.960	**0.001**	0.408	**0.001**	0.113
	(0.006)	(0.001)	(0.001)	(0.003)	(0.001)	(0.399)	(0.000)	(0.061)	(0.000)	(0.004)
					t distributed, $\nu = 7$					
sGPD^d	0.012	**0.062**	0.088	0.008	0.009	**0.111**	0.004	0.033	0.005	0.017
	(0.035)	(0.016)	(0.012)	(0.010)	(0.027)	(0.179)	(0.005)	(0.056)	(0.005)	(0.010)
sGPD^z	**0.006**	0.155	**0.086**	**0.006**	0.006	0.821	0.003	**0.033**	0.003	**0.015**
	(0.008)	(0.171)	(0.008)	(0.008)	(0.009)	(0.895)	(0.004)	(0.063)	(0.004)	(0.007)
sGPD^m	0.228	0.087	0.087	0.228	**0.003**	1.059	**0.001**	0.443	**0.001**	0.128
	(0.005)	(0.001)	(0.001)	(0.005)	(0.002)	(0.571)	(0.000)	(0.070)	(0.000)	(0.004)

function, and punish large errors more heavily than MAE. The MSEs are qualitatively similar to the MAE outcomes in terms of relative accuracy. Root MSEs are somewhat larger than the respective MAEs, suggesting that estimation errors are mildly right skewed. Again, the mixture density approach performs well, particularly when the tails are fat, but not extremely fat. In all three cases, the estimated static parameters tend to be close to the true parameters if the estimated model coincides with the DGP used for the simulation.

4 Time-varying tail risk and unconventional policies

We apply our score-driven GPD model to study the impact of two key and, arguably, controversial unconventional monetary policy measures adopted by the ECB during the euro area sovereign debt crisis on the tail risk associated with holding certain sovereign bonds. In practise, the risk of rapidly deteriorating government bond prices is not only borne by investors, but also by the dealers who make these markets. If uncertainty and tail risks become substantial, for example owing to debt sustainability or contagion concerns, then tail risks alone can force institutional investors and market makers to retreat, particularly if value-at-risk constraints are binding; see Vayanos and Vila (2009), and Adrian and Shin (2010).

4.1 ECB unconventional monetary policies: SMP and OMT

The absence of "depth and liquidity" in a subset of sovereign bond markets severely hinders a balanced, even transmission of a central bank's monetary policy stance across different countries in a monetary union. The SMP had the objective of helping to restore the monetary policy transmission mechanism by addressing the malfunctioning of certain government bond markets during the euro area sovereign debt crisis between 2010–2012; see, for instance, González-Páramo (2011). Implicit in the concept of malfunctioning markets is the notion that government bond yields can be unjustifiably high and volatile; see Eser et al. (2012) and Eser and Schwaab (2016). Government bond purchases within the SMP were made during a particularly severe sovereign debt crisis, when sovereign yields in several euro area countries were at a high, on the rise, and volatile. During this phase, the targeted securities met little private sector demand.

The introduction of the SMP was subject to significant controversy, both outside and within the Eurosystem, i.e., the ECB and all National Central Banks (NCBs). The extent of the controversy within the Eurosystem became evident with the resignation of the Bundesbank President in February 2011 and an ECB Executive Board member in September

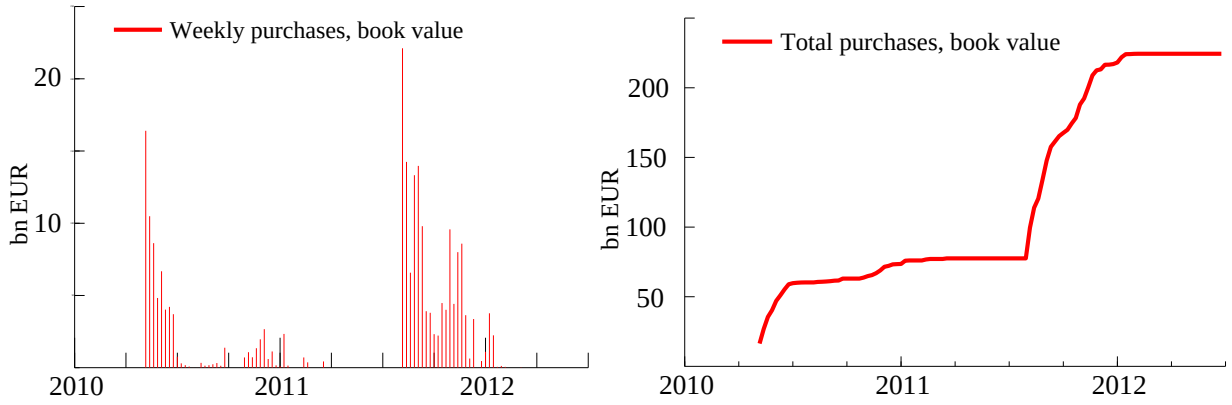

Figure 1: Weekly and total SMP purchase amounts.

The figure plots the book value of settled SMP purchases as of the end of a given week. We report weekly purchases across countries (left panel) as well as the cumulative amounts (right panel). Maturing amounts are excluded.

2011.[5] The SMP was replaced by the Outright Monetary Transactions (OMTs) program on 6 September 2012. The OMT is a program under which the ECB bank conducts purchases ("outright transactions") in secondary, sovereign bond markets, under certain conditions, of bonds issued by euro area member-states. The SMP and the OMTs are related but different programs, see Cœuré (2013).[6] No purchases have been made within the OMT program. Instead, the mere announcement of that program was sufficient to calm financial markets and contributed to ending the most acute phase of the sovereign debt crisis; see, for instance, ECB (2013), and Lucas et al. (2014, 2016).

Figure 1 plots weekly total SMP purchases across countries as well as their accumulated book value over time. Visibly, the weekly purchase data are unevenly spread over time. The SMP was announced on 10 May 2010 and focused on Greek, Irish, and Portuguese debt

[5] A cursory look at bond yields and bond purchases within the SMP can, as some suggested at the time, lead to the impression that the SMP was ineffective. In particular, yields were rising as purchases were taking place. Both Ghysels et al. (2016) and Eser and Schwaab (2016) note that yield changes and SMP purchase volumes at a daily frequency are positively correlated for most SMP countries. As a result, simple regression-based techniques that relate yield changes to purchase amounts lead to insignificant or even positive impact coefficient estimates. Among other significant concerns, being initially perceived as ineffective did not help the popularity of the program.

[6] Both SMP and OMT were (are) controversial monetary policy measures. The decision of the European Central Bank to enact OMT operations was not adopted unanimously. Critics pointed out that the program might erode the willingness of certain euro area member-states to implement reforms. In the meantime, the OMT has been challenged in the German Federal Constitutional Court, which in 2014 requested a preliminary ruling from the European Court of Justice.

securities. The program was extended to include Italian and Spanish bonds on 8 August 2011. Between 10 May 2010 and Spring 2012 there are long periods during which the SMP was open but inactive. Approximately €214 billion (bn) of bonds were acquired within the SMP between 2010 and early 2012. The SMP's daily cross-country breakdown of the purchase data is confidential at the time of writing. We use the confidential daily and country-specific data for this study.

Our data on bond yields is from Thomson Reuters. We consider the midpoint between continuous dealer quotes of ask and bid prices expressed in yields-to-maturity. Bond yields are sampled at the 15 minute frequency between 8AM and 6PM; see Ghysels et al. (2016) for a similar high-frequency approach. Figure 2 plots the yield-to-maturity of five-year benchmark bonds for five euro area countries between 04 January 2010 and 31 December 2012, at the 15 minute frequency. During the debt crisis, some yields exhibited occasional large and sudden moves, of up to 200 bps at a daily frequency, also leading to strong volatility spikes. Pronounced announcement effects of the SMP are visible in the yield data. Five-year yields dropped by -829 bps in Greece, -95 bps in Ireland, and -187 bps in Portugal on 10 May 2010; and by -90 bps in Spain and -62 bps in Italy on 8 August 2011, measured as the difference in five-year benchmark bond yields between Monday 6pm and the respective preceding Friday at 6pm. In addition, the credit event for Greek bonds on 09 March 2012 appears to have led to pronounced temporary spikes in yield levels and volatility in the other four markets.

4.2 Volatility and tail shape estimates

This section presents our volatility and tail shape estimates, and discusses the parameter estimates associated with the underlying models. We use a fairly straightforward t-GAS(1,1) volatility model to pre-filter our data before EVT estimation. The univariate volatility model is specified as

$$\begin{aligned} \tilde{y}_t &\sim \mathrm{t}(\tilde{y}_t; \sigma_t^2, \nu), \quad \ln(\sigma_t) = f_t^v, \\ f_{t+1}^v &= \omega_v + a_v \cdot s_{v,t} + b_v \cdot f_t^v, \end{aligned} \tag{12}$$

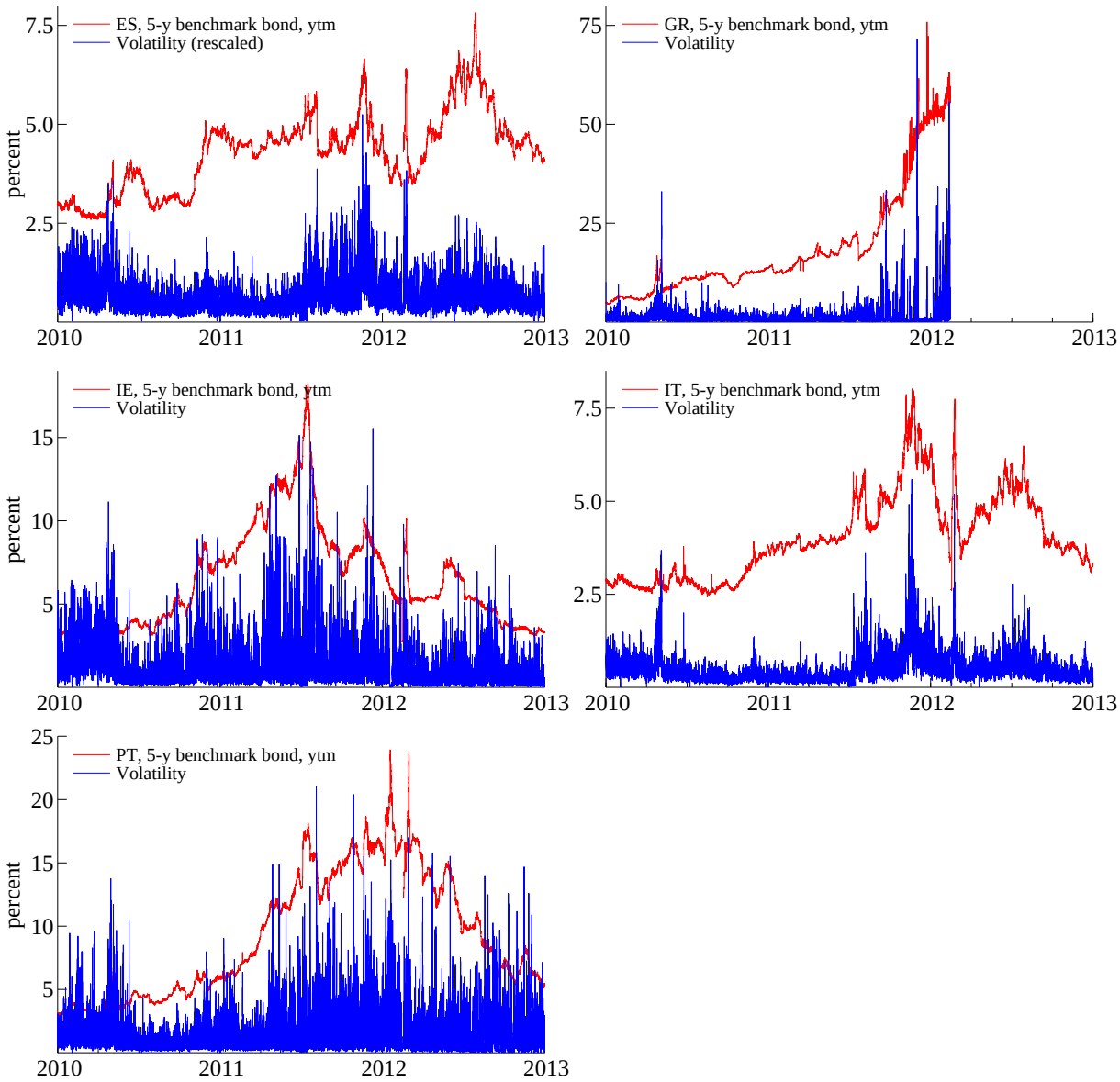

Figure 2: Five-year benchmark bond yields and volatility

Five-year benchmark bond yields and volatility estimates σ_t for Spain (ES), Greece (GR), Ireland (IE), Italy (IT), and Portugal (PT). Yields are in percentage points and are sampled at 15 minute intervals. The volatility estimates are based on the robust volatility model (12); see Table 3 for the respective parameter estimates. Volatilities are in percentage points, and re-scaled to match yields in terms of ranges to ensure visibility. Greek bonds discontinued trading after 02 March 2012, and experienced a credit event on 09 March 2012.

where $\tilde{y}_t$ is the recursively demeaned (but not yet devolatized) change in the quoted yield of a certain bond, ν is the degrees of freedom parameter, and $s_{v,t}$ is the scaled score from a t-distribution; see Creal et al. (2013) and Lucas et al. (2014) for details. Extending the

volatility factor specification with additional explanatory covariates along the lines of (11) is possible, but not considered here for simplicity. The key feature of the Student's t-GAS(1,1) model, which differentiates it from a conditionally Gaussian (GARCH) model, is a weighting term in its scaled score $s_{v,t}$ that lessens the impact of occasional extreme observations. Such extreme observations commonly occur during a sovereign debt crisis, and particularly at a high frequency. EVT estimation is based on POT observations $x_t = \max(\tilde{y}_t/\hat{\sigma}_t - \tau, 0)$, where $\hat{\sigma}_t$ is the volatility estimate from (12).

Figure 2 plots our volatility estimates at the 15 minute frequency viz-a-viz the respective bond yields. Volatility is high throughout 2010-2011 in Greece, Ireland, and Portugal, and peaks somewhat later around 2011Q4 in Italy and Spain. Greek bond volatility is most pronounced in the spring of 2012.

Figure 3 plots the filtered estimates of ξ_t. The tail shape is reported for different thresholds τ at the 10%, 5%, and 2.5% empirical quantile of x_t, respectively. We report estimates for different values of τ from a robustness perspective, and suggest to focus on the 5% empirical quantile (in red) as this value tends to do well in simulation settings; see Chavez-Demoulin and Embrechts (2010). Grey shaded areas in 2010 and 2011 mark periods of focussed SMP purchases in the respective markets, cf. Figure 1. The grey shaded area in 2012 marks the time after the announcement of the technical details of the ECB's OMT on 06 September 2012. The tail shape estimates suggest that periods of focussed asset purchases might be associated with reductions in the fatness of the right tail (i.e., ξ_t decreases), at least in some cases. The effects are the most visible for Greek bonds. These bonds exhibited the highest yields and were subject to a particularly elevated level of stress between 2010–2012. Specifically, the second quarter of 2010 appears to be an exception to the otherwise upwards trend in tail risk. Greek bonds ultimately experienced a credit event on 09 March 2012.

Table 3 (top panel) reports five sets of parameter estimates for the t-GAS volatility model (12). The estimates indicate that high-frequency yield changes are fat tailed, in all five markets. In all cases, the estimates of ν converge from above to 2.5, which we have chosen as a lower bound for that parameter to prevent numerical instability that may occur

Table 3: Parameter estimates

The top panel presents parameter estimates for five univariate t-GAS volatility models (12). Its final two columns report the parameter-implied mode 15 minute and daily volatility as $\bar{\sigma} = 100 \times \exp(\omega/(1-b_\nu))$ and $\sqrt{40} \times \bar{\sigma}$, respectively, expressed in basis points. Rows labeled ES, GR, IE, IT, and PT refer to Spanish, Greek, Irish, Italian, and Portuguese five-year bond yields. The estimation sample ranges from 04 January 2010 to 28 December 2012, except for Greece, for which the sample ends on 02 March 2012. Standard errors are in round brackets and are constructed from the numerical second derivatives of the log-likelihood function. The middle panel refers to the tail shape parameter model with parameter updates based on the mixture density (7); see (9) – (10). The final column reports the parameter-implied mode tail shape as $\bar{\xi} = \exp(\omega/(1-b))$. The bottom panel presents parameter estimates for the extended tail shape model (11) which includes additional variables as explanatory covariates.

t-GAS volatility model							
	ω_v	a_v	b_v	ν	LogLik	$\bar{\sigma}$	$\sqrt{40} \times \bar{\sigma}$
ES	-0.2360	0.2180	0.9377	2.5000	84766.1	2.26	14.32
	(0.0115)	(0.0052)	(0.0030)	(0.0000)			
GR	-0.2565	0.3236	0.9207	2.5000	39844.0	3.94	24.90
	(0.0113)	(0.0065)	(0.0034)	(0.0000)			
IE	-0.2644	0.3047	0.9283	2.5000	73240.1	2.50	15.83
	(0.0099)	(0.0051)	(0.0026)	(0.0000)			
IT	-0.1667	0.1854	0.9558	2.5000	86264.8	2.30	14.56
	(0.0094)	(0.0051)	(0.0024)	(0.0000)			
PT	-0.3146	0.3700	0.9071	2.5000	63207.3	3.38	21.40
	(0.0098)	(0.0055)	(0.0028)	(0.0000)			

Dynamic tail shape model (95%)					
	ω	a	b	LogLik	$\bar{\xi} = \exp \frac{\omega}{1-b}$
ES	-0.0453	0.0013	0.9652	-7421.7	0.27
	(0.0142)	(0.0015)	(0.0109)		
GR	0.0000	0.0029	1.0000	-9686.9	0.49
	(0.0001)	(0.0005)	(0.0001)		
IE	-0.0454	0.0000	0.9548	-10937.2	0.37
	(0.0178)	(0.0000)	(0.0177)		
IT	-0.0008	0.0016	0.9994	-8055.8	0.26
	(0.0005)	(0.0004)	(0.0004)		
PT	-0.0001	0.0017	0.9999	-11978.6	0.37
	(0.0001)	(0.0004)	(0.0001)		

Dynamic tail model (95%) with SMP volumes						
	ω	a	b	SMP_t	SMP_{t-1}	LogLik
ES	0.0000	0.0010	1.0000	0.0065	-0.0065	-7403.2
	(0.0001)	(0.0003)	(0.0001)	(0.0088)	(0.0088)	
GR	0.0000	0.0029	1.0000	0.0017	-0.0024	-9686.6
	(0.0001)	(0.0005)	(0.0001)	(0.0081)	(0.0081)	
IE	0.0000	0.0011	1.0000	-0.0331	0.0343	-10883.5
	(0.0000)	(0.0003)	(0.0000)	(0.0235)	(0.0235)	
IT	0.0000	0.0016	1.0000	0.0032	-0.0034	-8057.7
	(0.0001)	(0.0004)	(0.0001)	(0.0045)	(0.0045)	
PT	0.0000	0.0015	1.0000	0.0120	-0.0146	-11977.5
	(0.0000)	(0.0003)	(0.0000)	(0.0167)	(0.0167)	

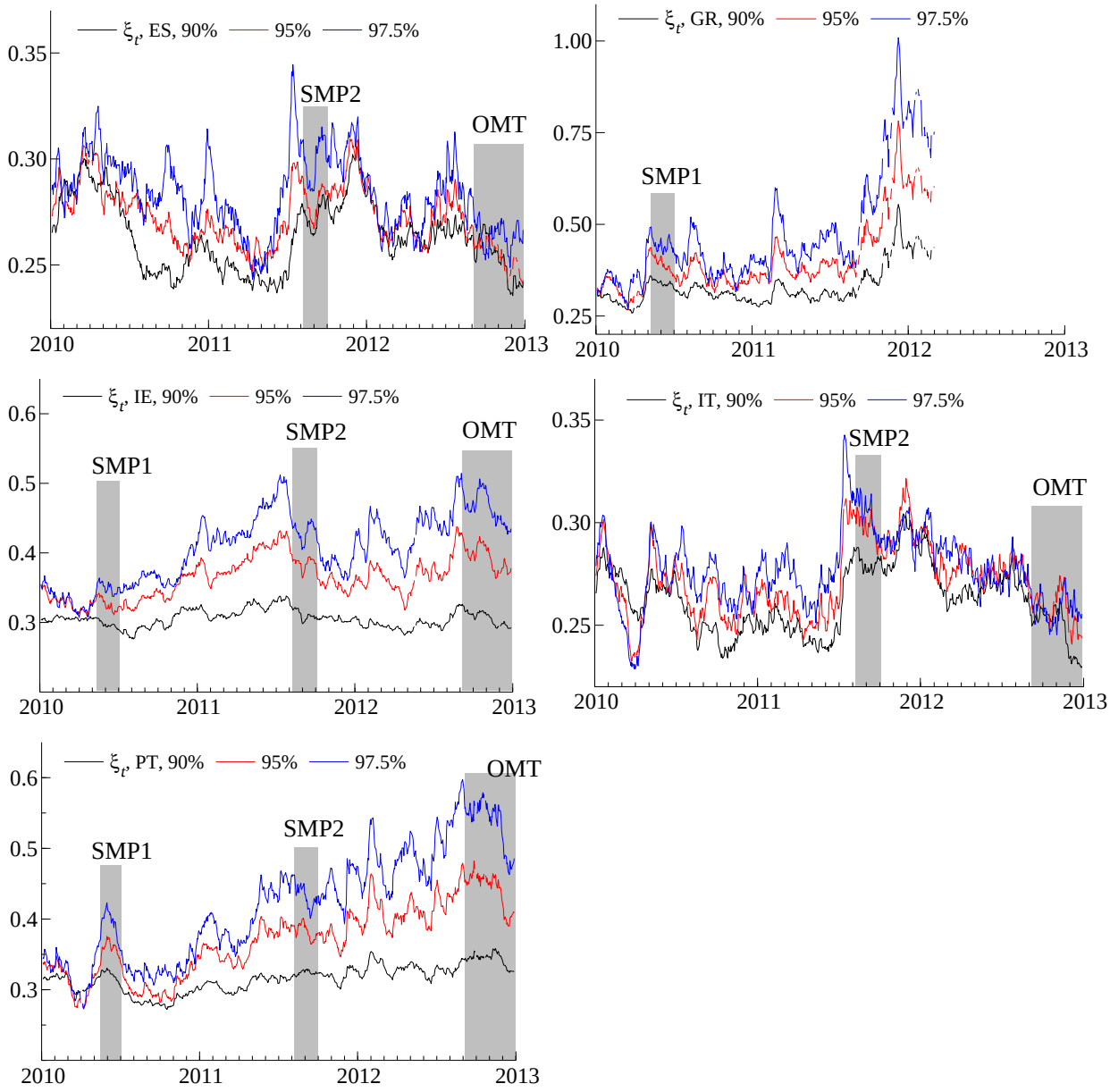

Figure 3: Tail risk dynamics in five euro area countries

Estimates of the time-varying tail shape parameter ξ_t at different levels of τ, corresponding to the 10%, 5%, and 2.5% quantile, for Spain (ES), Greece (GR), Ireland (IE), Italy (IT), and Portugal (PT). Daily estimates are obtained as the median value of the estimates at the 15 minute frequency. Shaded areas in 2010 and 2011 refer to frequent asset purchases within the SMP; see Figure 1. The shared area in late 2012 marks the period after the announcement of the technical details of the ECB's OMT program on 06 September 2012. Greek bonds discontinued trading after 02 March 2012, and experienced a credit event on 09 March 2012.

in the estimation as $\nu \downarrow 2$.[7] In addition, the volatility processes are fairly persistent, with

[7]EVT estimates are fairly robust to changes in the specification of the volatility model that is used to pre-filter the data; see Rocco (2014). Requiring $\nu \geq 2.5$ leads to a relevant robustification of the volatility filter; see Harvey (2013).

$b_v > 0.9$ in all cases.

The middle panel of Table 3 presents the parameter estimates for our baseline score-driven tail shape model (3). We focus on the mixture approach (7) – (10), as this approach performed well in our simulations as reported in Section 3, and allows us to obtain an estimate of ξ_t at each point in time. The tail shape parameter estimates indicate fat tails, with mode values $\bar{\xi} = \exp(\omega/(1-b))$ reported in the last column of the bottom panel of Table 3. Overall, tail fatness is in line with what is suggested by the t-GAS volatility models, and suggests that t-distributions with $\nu \approx 2-3$ are appropriate for modeling changes in euro area bond yields at 15-minute intervals between 2010–2012. The tail shape processes are persistent, with typical values of $b > 0.95$.

Table 3 also presents the estimation results for the GAS-X specification (11) which allows for additional explanatory covariates (bottom panel). We obtain mixed evidence regarding the importance of SMP variables for explaining time variation in tail shape. On the one hand, none of the coefficients for SMP variables are statistically significant according to their t-values. In addition, three (of five) log-likelihoods are only marginally higher than for specification (3). This outcome is robust to considering changes in purchases instead of levels, and to replacing the purchase amounts with dummies indicating the presence of the ECB in the respective markets. On the other hand, the additional SMP variables leads to significant increases in log-likelihood in two cases (Spanish and Irish bonds). We conclude that the direct inclusion of SMP variables does not significantly improve the fit of the dynamic tail index model in all cases. This finding does not necessarily imply that purchases had no effect on the tail shape. Instead, appropriate control covariates may be required (see footnote 5).

4.3 Impact on tail shape

We quantify the impact of SMP purchases on tail shape by estimating univariate time series regressions at the country (bond) level,

$$\begin{aligned} \hat{\xi}_t^D &= \beta_0 + \beta_1 \hat{\xi}_{t-1}^D + \beta_2 \mathrm{D}_t^{10\mathrm{May}} + \beta_3 \mathrm{D}_{t-1}^{10\mathrm{May}} + \beta_4 \mathrm{D}_t^{08\mathrm{Aug}} + \beta_5 \mathrm{D}_{t-1}^{08\mathrm{Aug}} \\ &+ \beta_6 \mathrm{SMP}_t + \beta_7 \mathrm{SMP}_{t-1} + \beta_8 \mathrm{SMP}_{t-2} + \beta_9 \mathrm{D}_t^{\mathrm{OMT}} + \beta_{10} \mathrm{D}_{t-1}^{\mathrm{OMT}} + \epsilon_t, \end{aligned} \tag{13}$$

where $\hat{\xi}_t^D = 1000 \times (\hat{\xi}_t^R - \hat{\xi}_t^L)$ is the scaled-up difference between the right (bad) tail shape estimate $\hat{\xi}_t^R$ and the tail shape estimate $\hat{\xi}_t^L$ for the left (good) tail. The respective threshold value τ is taken as the empirical 5% percentile, implying two positive POT values per day on average. Regression (13) is specified at the daily frequency, where the regressand is sampled at 6pm. $\mathrm{D}_t^{10\mathrm{May}}$ and $\mathrm{D}_t^{08\mathrm{Aug}}$ are dummy variables capturing SMP announcement effects on 10 May 2010 and 08 August 2011, respectively. We include lagged effects to allow for a delay in measured impact. SMP_t denotes the total amount spent on SMP asset purchases, in €billion of par value, in a certain bond market (all maturities) on intervention day t. Finally, the dummy variable $\mathrm{D}_t^{\mathrm{OMT}}$ marks the ECB's announcement of the technical details of its OMT program on 06 September 2012.

Considering the difference $\hat{\xi}_t^R - \hat{\xi}_t^L$ treats $\hat{\xi}_t^L$ as a control (benchmark) variable. The left tail shape explains some of the time variation in the right tail shape, for example owing to shared exposure to common uncertainty about debt sustainability and political outcomes. Simultaneously, the left tail shape is unlikely to be impacted by SMP asset purchases. The ECB's first SMP-related press release on 10 May 2010 clarified that purchased bonds would be retired on the ECB balance sheet until the bonds mature. The ECB never sold (nor lent out) any government bonds purchased within the SMP. As a result, the SMP was a 'one-sided' program, and its purchases during the debt crisis are best pictured as 'leaning against' the potential of sharply rising yields during the sovereign debt crisis.[8] If the left tail shape were to decline following an SMP intervention, in line with a reduction in uncertainty, then the impact estimates based on (13) constitute a conservative lower bound.

Regression (13) uses a generated regressand; see, for example, Pagan (1984) for a discussion. This means that t-statistics based on OLS standard errors may be inflated by an unknown amount. In addition, differences in sampling error in the first step may lead to heteroscedastic error terms in the second step; see Lewis and Linzer (2005). The second issue is unlikely to be a problem in our setting, as our EVT-based inference is performed on devolatized data x_t. Robust standard errors may mitigate the bias in standard errors

[8] We experimented with including SMP variables into the specification of the left tail shape via (11). The respective SMP coefficient estimates, as well as increments in log-likelihood, are insignificant, with the exception of lagged purchases for the Irish five-year bond.

to some extent; see again Lewis and Linzer (2005). We nevertheless suggest to interpret the parameter standard errors associated with regression (13) with caution, and to apply a higher-than-usual thresholds to the reported Heteroskedastic and Autocorrelation Consistent (HAC) t-statistics. Parameter estimates in regression (13) are consistent under fairly weak assumptions.

The top panel in Table 4 reports the parameter estimates for (13) obtained by least squares regression. The estimates suggest that the announcement of ECB asset purchases on 10 May 2010 and 08 August 2011 lowered the tail risk of holding sovereign bonds in all countries (except possibly Italy). The initial announcement on 10 May appears to have had a relatively stronger effect than the re-announcement and extension on 08 August 2011. The impact coefficients for actual purchases may be statistically significant in some cases; the economic magnitude of these impacts, however, is small and arguably negligible. (Recall that tail shape differences are scaled up by a factor of 1000, and purchases are scaled in €bn.) Changes in tail risk tend to be associated with lagged, not contemporaneous, purchases. This may reflect the fact that $\hat{\xi}_t^R$ is filtered from sparse data. Future (smaller) exceedances are required to lower the dynamic tail shape parameter. The tail shape differences are persistent even at the daily frequency, with autoregressive coefficients close to one. This pronounced persistence suggests to also consider time differences; see specification (14) below. The OMT program is associated with falling tail risk, particularly for Spanish and Irish bonds. No estimate for OMT impact is available for Greek benchmark bonds, as these discontinued trading in March 2012.

To give the filtered tail shape parameter more time to adjust to contemporaneous ECB actions, and to accommodate the autocorrelation in the tail shape estimates, we also consider two-day (34 hour) tail differences as the dependent variable. This means we compare the tail shape estimates at the end of day t at 6pm with the estimate at the start of day $t-1$ at 8am. We benchmark the time difference by the corresponding difference for the left-hand tail, again assuming that asset purchases affect only the right-hand tail. Specifically, we construct scaled up differences-in-differences $\hat{\xi}_t^{DiD} = 1000 \times \Big((\hat{\xi}^R_{t,6pm} - \hat{\xi}^R_{t-1,8am}) - (\hat{\xi}^L_{t,6pm} - \hat{\xi}^L_{t-1,8am}) \Big)$,

Table 4: Regression estimates for tail risk differences

The top, middle, and bottom panel report least squares parameter estimates for univariate time series regressions (13), (14), and (17), respectively. Rows ES, GR, IE, IT, and PT refer to parameter estimates for Spanish, Greek, Irish, Italian, and Portuguese five-year benchmark bonds. Parameter t-values are in square brackets and are based on Newey-West HAC standard errors.

	const.	$\hat{\xi}^D_{t-1}$	$\mathrm{D}_t^{\mathrm{10May}}$	$\mathrm{D}_{t-1}^{\mathrm{10May}}$	$\mathrm{D}_t^{\mathrm{08Aug}}$	$\mathrm{D}_{t-1}^{\mathrm{08Aug}}$	SMP_t	SMP_{t-1}	SMP_{t-2}	$\mathrm{D}_t^{\mathrm{OMT}}$	$\mathrm{D}_{t-1}^{\mathrm{OMT}}$	R^2
ES	0.34	0.97	-4.67	-0.52	-10.68	-16.22	0.00	0.00	-0.00	-12.46	-4.59	0.94
	[1.8]	[98.4]	[-33.6]	[-3.5]	[-2.2]	[-4.5]	[1.9]	[0.4]	[-4.5]	[-48.0]	[-12.6]	
GR	-0.03	0.99	-0.25	-0.25	0.17	0.05	0.00	-0.00	0.00	-	-	0.99
	[-2.3]	[90.1]	[-2.8]	[-3.0]	[13.8]	[3.9]	[1.4]	[-3.0]	[1.1]	-	-	
IE	0.32	0.98	-20.48	-19.49	-8.85	-1.06	0.01	0.00	-0.00	-6.64	-8.54	0.97
	[1.20]	[125.]	[-4.9]	[-3.6]	[-17.4]	[-2.3]	[3.1]	[0.5]	[-3.0]	[-24.0]	[-34.6]	
IT	-0.00	0.98	0.18	0.13	0.14	-0.04	-0.00	0.00	0.00	0.00	0.04	0.97
	[-0.5]	[122.]	[39.2]	[37.6]	[2.8]	[-0.8]	[-1.3]	[1.4]	[1.2]	[1.4]	[12.7]	
PT	0.49	0.98	-9.58	-3.16	-7.35	-10.40	0.00	-0.00	0.00	4.94	-2.26	0.97
	[1.2]	[137.]	[-3.1]	[-0.5]	[-12.8]	[-18.6]	[2.8]	[-1.0]	[1.2]	[19.2]	[-9.1]	

	const.	$\mathrm{D}_t^{\mathrm{10May}}$	$\mathrm{D}_{t-1}^{\mathrm{10May}}$	$\mathrm{D}_t^{\mathrm{08Aug}}$	$\mathrm{D}_{t-1}^{\mathrm{08Aug}}$	SMP_t	SMP_{t-1}	SMP_{t-2}	$\mathrm{D}_t^{\mathrm{OMT}}$	$\mathrm{D}_{t-1}^{\mathrm{OMT}}$	R^2
ES	-0.15	-3.46	-3.73	-22.78	-21.90	2.35	0.73	-2.44	-16.43	-13.33	0.04
	[-0.6]	[-13.0]	[-14.1]	[-3.6]	[-4.7]	[2.2]	[0.8]	[-5.1]	[-62.0]	[-50.3]	
GR	-0.03	-0.33	-0.55	0.29	0.02	0.01	-0.02	-0.02			0.01
	[-1.1]	[-2.4]	[-3.3]	[11.4]	[0.6]	[0.3]	[-0.7]	[-0.9]			
IE	-0.08	-15.43	-30.30	-9.72	-10.80	7.78	4.67	-6.54	-12.13	-20.26	0.02
	[-0.2]	[-1.8]	[-2.8]	[-8.7]	[-15.5]	[1.5]	[1.6]	[-3.5]	[-29.3]	[-48.9]	
IT	0.00	0.24	0.23	0.16	0.05	-0.01	0.01	0.00	0.02	0.00	0.02
	[-0.5]	[53.6]	[50.0]	[1.6]	[0.7]	[-0.8]	[1.1]	[0.6]	[3.9]	[-0.6]	
PT	-0.12	-6.84	-13.98	-17.29	-19.07	4.55	-0.70	-0.92	9.34	-12.08	0.02
	[-0.3]	[-1.0]	[-2.0]	[-15.0]	[-25.3]	[1.5]	[-0.4]	[-0.5]	[19.5]	[-25.2]	

	const.	$\mathrm{D}_t^{\mathrm{10May}}$	$\mathrm{D}_{t-1}^{\mathrm{10May}}$	$\mathrm{D}_t^{\mathrm{08Aug}}$	$\mathrm{D}_{t-1}^{\mathrm{08Aug}}$	SMP_t	SMP_{t-1}	$\mathrm{D}_t^{\mathrm{OMT}}$	$\mathrm{D}_{t-1}^{\mathrm{OMT}}$	R^2
ES	0.00	-1.26	-0.28	0.25	-1.23	-0.00	0.00	-0.66	0.01	0.03
	[0.1]	[-163.]	[-36.3]	[0.2]	[-1.3]	[-0.2]	[0.4]	[-85.7]	[0.9]	
GR	0.14	-9.92	4.56	-1.1	-0.82	-0.00	0.00	-	-	0.01
	[0.8]	[-1.5]	[1.4]	[-5.9]	[-4.6]	[-1.1]	[0.4]	-	-	
IE	-0.02	-1.65	-1.80	-2.21	8.41	0.00	-0.00	-1.55	-0.15	0.01
	[-0.2]	[-0.4]	[-0.4]	[-6.4]	[43.1]	[0.5]	[-0.5]	[-21.4]	[-2.0]	
IT	0.01	-2.00	-0.19	1.09	-1.63	-0.00	0.00	0.69	-0.47	0.03
	[0.6]	[232.]	[-22.3]	[1.3]	[-2.8]	[-0.9]	[0.9]	[80.0]	[-54.2]	
PT	-0.00	2.41	-3.47	-6.74	3.10	-0.00	0.00	7.10	-7.88	0.01
	[-0.0]	[0.4]	[-1.9]	[-20.2]	[8.2]	[-0.2]	[0.4]	[42.3]	[-46.9]	

and relate these to unconventional monetary policies as

$$\begin{aligned}\hat{\xi}_t^{DiD} &= \beta_0 + \beta_1 \mathrm{D}_t^{\mathrm{10May}} + \beta_2 \mathrm{D}_{t-1}^{\mathrm{10May}} + \beta_3 \mathrm{D}_t^{\mathrm{08Aug}} + \beta_4 \mathrm{D}_{t-1}^{\mathrm{08Aug}} \\ &+ \beta_5 \mathrm{SMP}_t + \beta_6 \mathrm{SMP}_{t-1} + \beta_7 \mathrm{SMP}_{t-2} + \beta_8 \mathrm{D}_t^{\mathrm{OMT}} + \beta_9 \mathrm{D}_{t-1}^{\mathrm{OMT}} + \epsilon_t, \qquad (14)\end{aligned}$$

where right-hand side variables are defined as in (13).

The middle panel of Table 4 presents the respective least squares parameter estimates. The main results are similar to the outcome reported in the top panel. We again document clear announcement effects regarding SMP asset purchases for both the 10 May 2010 and 08 August 2011 statement (columns 3–4, and 5–6, respectively). Similarly, the OMT dummy variable is negatively related to time-variation in the tail shape parameter (except Italy; columns 10–11). Conversely, the implementation of the purchases on a day-to-day basis does not appear to have had an economically meaningful additional impact on tail shape (columns 7–9), as the row sums of the respective coefficient estimates are close to zero. For Italy, no entry is both negative and statistically significant. This negative finding is approximately in line with the empirical results in Ghysels et al. (2016) and Eser and Schwaab (2016), where the smallest impact estimate (per €1 bn) on the conditional mean is also obtained for Italian bonds. We conclude that the announcement of ECB unconventional policy measures, such as the SMP and OMT, helped lower the tail shape associated with holding certain sovereign bonds between 2010–2012. By contrast, the implementation of announced purchases within the SMP does not appear to have had a strong effect on tail shape.

4.4 Impact on market risk

This section quantifies the impact of SMP purchases on the market risk associated with holding certain SMP government bonds between 2010–2013. The focus on market risk also allows us to revisit the economic significance of unconventional monetary policies such as the ECB's SMP and OMT. Specifically, we consider the Value-at-Risk (VaR) and Expected Shortfall (ExS) 15 minutes ahead and at a 99% confidence level. The measurement of market risk is a major application of EVT methods in practise; see McNeil et al. (2010).

A useful relationship between the GPD and excess loss measures is presented in McNeil and Frey (2000); see also Rocco (2014). In our setting, an EVT-based estimate of the VaR

of y_t at quantile γ can be obtained as

$$\mathrm{VaR}_t^{\gamma}(Y) = \hat{\sigma}_t \tau + \frac{\hat{\sigma}_t}{\hat{\xi}_t} \left[\left(\frac{N}{N_\tau} (1-\gamma)^{-\hat{\xi}_t} \right) - 1 \right], \tag{15}$$

where $\hat{\sigma}_t$ is obtained from (12), ξ_t is as above, and τ is fixed for a given data sample of size $N = t$ at time t. As the sample size increases, time variation in τ is present but also negligible, as it refers to devolatized data x_t from a growing sample at a high frequency. For any sample of size $N = t$, we observe N_τ non-zero observation for x_t. The corresponding Expected Shortfall is the average VaR in the tail, see McNeil, Frey, and Embrechts (2010, Chapter 2). Assuming that $\xi_t < 1$, an closed-form expression is available as

$$\mathrm{ExS}_t^{\gamma}(Y) = \frac{1}{1-\gamma} \int_{\gamma}^{1} \mathrm{VaR}_t^{\tau}(Y) \mathrm{d}\tau = \frac{\mathrm{VaR}_t^{\gamma}(Y)}{1-\hat{\xi}_t} + \frac{\hat{\sigma}_t (1 - \hat{\xi}_t \tau)}{1-\hat{\xi}_t}. \tag{16}$$

The $\mathrm{ExS}_t^{\gamma}(Y)$ (16) is strictly higher than the $\mathrm{VaR}_t^{\gamma}(Y)$ (15) at the same confidence level, as it "looks further into the tail" of suddenly rising yields. In addition, it can be shown that the ratio $\mathrm{ExS}_t^{\gamma}(Y)/\mathrm{VaR}_t^{\gamma}(Y)$ is monotonously increasing in ξ_t for $\gamma \to 1$.

Figure 4 plots our time series estimates of VaR and Expected Shortfall at a 99% confidence level for five SMP benchmark bonds. We focus on three findings. First, government bonds differed substantially in terms of their tail risk at any time during the euro area sovereign debt crisis. Italian and Spanish bonds had the lowest estimated Expected Shortfall, with a risk of an increase of up to approximately 50 bps on average within 15 minutes at the 99% confidence level. Irish and Portuguese bonds were intermediate cases, with a 15-minute 99% Expected Shortfall of up to 150 bps. Finally, Greek bonds had the highest estimated 15-minute Expected Shortfall of up to 300 bps, particularly in the period leading up to the eventual credit event in March 2012.

Second, Figure 4 also reveals a different timing of the maximum amount of market risk in each market segment. The highest tail risks are observed relatively late in Spain and Italy, with pronounced peaks in 2011Q4. By contrast, elevated market stress is visible for Greek, Irish and Portuguese bonds already much earlier, between 2010 – 2011. This is

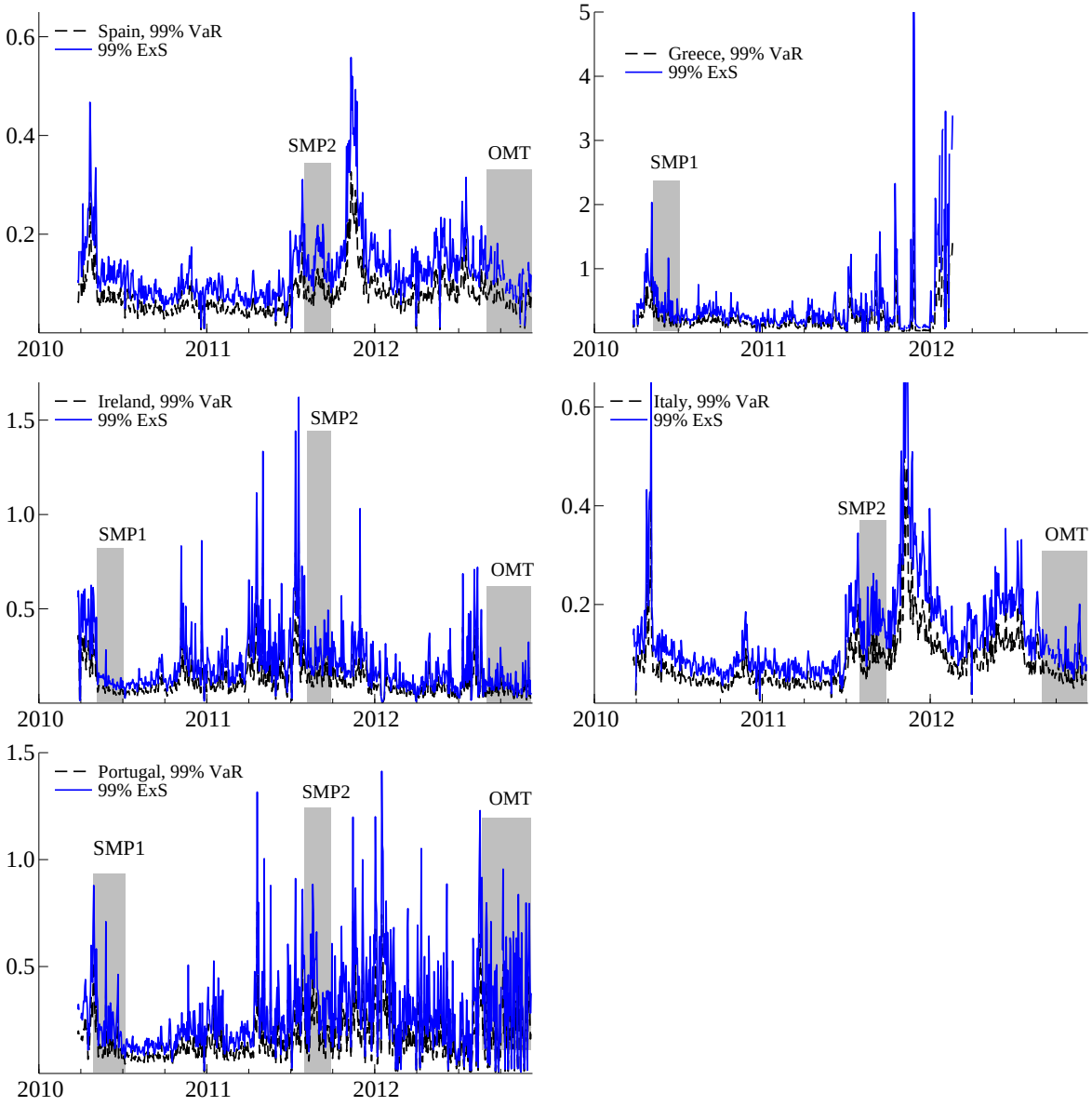

Figure 4: VaR and ExS estimates for five SMP bonds

Value-at-Risk (VaR) and Expected Shortfall (ExS) estimates for five-year benchmark government bonds for Spain (ES), Greece (GR), Ireland (IE), Italy (IT), and Portugal (PT). The VaR and ES are at a 99% confidence level. Shaded areas correspond to policy interventions; cf. Figure 3. Data between 01 January and 30 March 2010 are used to initiate the threshold τ, and are therefore not reported. The panels plot the daily median of the 15 minute estimates.

approximately in line with standard accounts of the debt crisis; see, for example, Cœuré (2013), according to which smaller countries in the periphery of the euro area were affected first, and larger countries such as Italy and Spain were affected later. Interestingly, outright purchases within the SMP appear to have reduced the VaR and Expected Shortfall of SMP bonds; particularly for Greek, Irish, and Portuguese bonds during 2010 and 2011.

To quantify the impact of ECB asset purchases on market risk we follow the same empirical strategy as in Section 4.3. We again benchmark the right (bad) tail value to its left-tail value, and consider daily differences, as $\text{ExS}_t^{DiD} = (\text{ExS}_t^R - \text{ExS}_{t-1}^R) - (\text{ExS}_t^L - \text{ExS}_{t-1}^L)$. ExS_t^{DiD} is measured in basis points, and sampled at 6pm. We relate these differences in market risk to ECB unconventional policies,

$$\begin{aligned} \text{ExS}_t^{DiD} &= \beta_0 + \beta_1 \text{D}_t^{\text{10May}} + \beta_2 \text{D}_{t-1}^{\text{10May}} + \beta_3 \text{D}_t^{\text{08Aug}} + \beta_4 \text{D}_{t-1}^{\text{08Aug}} \\ &+ \beta_5 \text{SMP}_t + \beta_6 \text{SMP}_{t-1} + \beta_7 \text{D}_t^{\text{OMT}} + \beta_8 \text{D}_{t-1}^{\text{OMT}} + \epsilon_t, \end{aligned} \tag{17}$$

where again right-hand side variables are defined below (13). Impact estimates from specification (17) are conservative if unconventional policies move the left-hand Expected Shortfall as well. This is the case, by construction, if unconventional policies had an impact on the conditional second moment. This is likely the case. For example, Ghysels et al. (2016) find that SMP purchases had a negative impact on the conditional variances at a high frequency.

The bottom panel of Table 4 reports the regression outcomes. The announcement of the SMP on 10 May 2010 reduced the 15-minute Expected Shortfall from holding five-year government benchmark bonds by approximately -1.1 (PT), -3.5 (IE), and up to -5.4 bps (GR). Reductions in Expected Shortfall can also be observed for Spain and Italy at this time, with impacts of approximately -1.5 and -2.2 bps, respectively. These are economically meaningful reductions given the magnitudes of market risk at these times; see Figure 4. The respective 15-minute Expected Shortfalls range from approximately 20 to 40 bps (Ireland, Italy, and Spain), and up to 150 bps (Greece), on average on the ten days preceding the 10 May 2010 announcement. The re-announcement and extension of the SMP on 08 August 2011 reduced the 15-minute Expected Shortfall of Spanish and Italian bonds by approximately -1

bps. As a result, the re-announcement effects are generally smaller than those for the initial announcement on 10 May 2010. This finding could be due to a combination of two effects. First, purchases following the 8 August 2011 mainly focused on the Italian and Spanish debt markets, which were relatively less stressed, as well as larger and deeper. Second, based on the fact that the SMP interventions that began in May 2010 were toned down after a while, it is possible that some market participants expected a similar development after the reactivation of the SMP.

The bottom panel of Table 4 provides no evidence that the implementation of announced SMP purchases reduced market risk (columns 7–8). The respective impact estimates are statistically and economically insignificant. As a caveat, market risk may still decline though a reduction in the conditional variance of bond yields; see Ghysels et al. (2016). Finally, the risk impact of the OMT announcement on 06 September 2012 ranges between zero (Italy) and approximately -2 bps (Ireland). This event study-type impact is significant, but likely understates the cumulative effect of OMT on sovereign tail risks; see Figure 4 and Lucas et al. (2014). The regression estimates for VaR differences are qualitatively similar and therefore omitted. We conclude that ECB unconventional policies likely contributed towards mitigating high tail risk in government bond markets during the sovereign debt crisis between 2010-2012. While there is little evidence that the implementation of SMP purchases affected measured market risks, the announcements of both SMP and OMT led to meaningful reductions. By extension, these programs contributed to restoring the "depth and liquidity" of certain bond markets that were the most affected by the crisis, by helping market makers to remain active during turbulent times.

5 Conclusion

This paper introduced time variation into the tail shape parameter of the Generalized Pareto Distribution, yielding a novel observation-driven model. Specifically, our modeling framework allows us to track the time variation in the tail index of time series observations from a wide class of fat-tailed distributions. In the empirical application, we demonstrated that

two controversial unconventional monetary policies adopted by the ECB during the euro area sovereign debt crisis lowered the tail shape and mitigated the extreme market risks associated with holding certain sovereign bonds between 2010–2012.

Appendix A1: Score and scaling function for a GPD random variable

This section derives (4) – (5). Recall the GPD pdf

$$p(x_t;\delta,\xi_t)=\frac{1}{\delta}\left(1+\xi_t\frac{x_t}{\delta}\right)^{-\frac{1}{\xi_t}-1},$$

and that the respective log-likelihood is given by (2) as $l(x_t;\delta,\xi_t)=-\ln(\delta)-\left(1+\frac{1}{\xi_t}\right)\ln\left(1+\xi_t\frac{x_t}{\delta}\right)$, where $\delta>0$, $\xi_t>0$, $x_t>0$, and $\xi_t=\exp(f_t)$. The score function (4) is straightforward, and is obtained as

$$\begin{aligned}\nabla_t &= \frac{\partial l(x_t;\delta,\xi_t)}{\partial f_t}=\frac{\partial l(x_t;\delta,\xi_t)}{\partial \xi_t}\cdot\frac{\mathrm{d}\xi_t}{\mathrm{d}f_t},\\ \frac{\partial l(x_t;\delta,\xi_t)}{\partial \xi_t} &= \frac{1}{\xi_t^2}\ln\left(1+\xi_t\frac{x_t}{\delta}\right)-\left(1+\frac{1}{\xi_t}\right)\frac{x_t}{\delta+\xi_t x_t},\\ \frac{\mathrm{d}\xi_t}{\mathrm{d}f_t} &= \exp(f_t).\end{aligned}$$

The score is zero in expectation if the model is well-specified; see Creal et al. (2013), implying

$$\int_0^\infty\frac{1}{\xi_t^2}\ln\left(1+\xi_t\frac{x_t}{\delta}\right)p(x_t;\delta,\xi_t)\mathrm{d}x_t=\int_0^\infty\left(1+\frac{1}{\xi_t}\right)\frac{x_t}{\delta+\xi_t x_t}p(x_t;\delta,\xi_t)\mathrm{d}x_t. \tag{A1}$$

The scaling function is chosen as the inverse conditional Fisher information of the GPD,

$$\mathcal{S}_t=\mathrm{E}[\nabla_t^2|\mathcal{F}_{t-1};f_t,\psi]^{-1}=\mathrm{E}\left[\left(\frac{\partial l(x_t;\delta,\xi_t)}{\partial\xi_t}\right)^2\left(\frac{\mathrm{d}\xi_t}{\mathrm{d}f_t}\right)^2\right]^{-1}=\mathrm{E}\left[-\frac{\partial^2 l(x_t;\delta,\xi_t)}{\partial\xi_t^2}\right]^{-1}\exp(-2f_t),$$

where the last equality sign uses a standard result. The expected negative second derivative is

$$\begin{aligned}
\mathrm{E}\left[-\frac{\partial^2 l(x_t;\delta,\xi_t)}{\partial \xi_t^2}\right] &= -\int_0^\infty \left[\left(1+\frac{1}{\xi_t}\right)\frac{x_t^2}{(\delta+\xi_t x_t)^2}+\frac{2}{\xi_t^2}\frac{x_t}{\delta+\xi_t x_t}-\frac{2}{\xi_t^3}\ln\left(1+\xi_t\frac{x_t}{\delta}\right)\right]p(x_t;\delta,\xi_t)\mathrm{d}x_t \\
&= -\int_0^\infty \left[\left(1+\frac{1}{\xi_t}\right)\frac{x_t^2}{(\delta+\xi_t x_t)^2}+\frac{2}{\xi_t^2}\frac{x_t}{\delta+\xi_t x_t}-\frac{2}{\xi_t}\left(1+\frac{1}{\xi_t}\right)\frac{x_t}{\delta+\xi_t x_t}\right]p(x_t;\delta,\xi_t)\mathrm{d}x_t \\
&= -\int_0^\infty \left[\left(1+\frac{1}{\xi_t}\right)\frac{x_t^2/\delta^2}{(1+\xi_t x_t/\delta)^2}-\frac{2}{\xi_t}\frac{x_t/\delta}{1+\xi_t x_t/\delta}\right]\frac{1}{\delta}\left(1+\xi_t\frac{x_t}{\delta}\right)^{-\frac{1}{\xi_t}-1}\mathrm{d}x_t \\
&= -\int_0^\infty \left[\left(\frac{1+\xi_t}{\xi_t^3}\right)\frac{\xi_t^2 x_t^2/\delta^2}{(1+\xi_t x_t/\delta)^2}-\frac{2}{\xi_t^2}\frac{\xi_t x_t/\delta}{1+\xi_t x_t/\delta}\right]\frac{1}{\delta}\left(1+\xi_t\frac{x_t}{\delta}\right)^{-\frac{1}{\xi_t}-1}\mathrm{d}x_t \\
&= -\frac{1+\xi_t}{\xi_t^4}\int_1^\infty (u_t-1)^2 u_t^{-1/\xi_t-3}\mathrm{d}u_t+\frac{2}{\xi_t^3}\int_1^\infty (u_t-1)u_t^{-1/\xi_t-2}\mathrm{d}u_t, \qquad \text{(A2)}
\end{aligned}$$

where we used (A1) in the second line, and where the last equality comes from a change of variable substituting $u_t = 1+\xi_t x_t/\delta$.

The two integrals in (A2) can be treated as scaled up first moments $\mathrm{E}(u_t)$. To see this, note that the new random variable u_t is Pareto (Type 1) distributed, with pdf

$$\tilde{p}(u_t;a_t,b) = \frac{a_t b^{a_t}}{{u_t}^{a_t+1}}, \qquad u_t > 1, \qquad \text{(A3)}$$

with nth un-centered moment available as

$$\mathrm{E}(u_t^n) = \frac{a_t b^n}{a_t - n}. \qquad \text{(A4)}$$

The first integral in (A2) corresponds to $\tilde{p}(u_t;1/\xi_t+2,1)$, while the second integral corresponds to $\tilde{p}(u_t;1/\xi_t+1,1)$. This implies that

$$\begin{aligned}
-\frac{1+\xi_t}{\xi_t^4}\int_1^\infty (u_t-1)^2 u_t^{-1/\xi_t-3}\mathrm{d}u_t &= \frac{-2}{\xi_t(1+2\xi_t)} \\
\frac{2}{\xi_t^3}\int_1^\infty (u_t-1)u_t^{-1/\xi_t-2}\mathrm{d}u_t &= \frac{2}{\xi_t(1+\xi_t)}.
\end{aligned}$$

Adding terms and inverting, we obtain the scaling function (5) in closed form as

$$\mathcal{S}_t = \frac{(1+2\xi_t)(1+\xi_t)}{2}\exp\left(-2f_t\right) = \frac{(1+2\xi_t)(1+\xi_t)}{2\xi_t^2}.$$

Appendix A2: Score and scaling function for a mixture of a GPD with a point mass at zero

This section derives (9) – (10). Recall that the mixture GPD density (7) has a point mass at zero and is given by

$$\phi(x_t;\delta,\xi_t) = \mathrm{I}(x_t>0)\left[(1+\tau)^{-\frac{1}{\xi_t}}\frac{1}{\delta}\left(1+\xi_t\frac{x_t}{\delta}\right)^{-\frac{1}{\xi_t}-1}\right] + \mathrm{I}(x_t=0)\left(1-(1+\tau)^{-\frac{1}{\xi_t}}\right).$$

The respective log-likelihood (8) is given by

$$\begin{aligned}\ell(x_t;\delta,\xi_t) &= \mathrm{I}(x_t>0)\left[-\frac{1}{\xi_t}\ln(1+\tau) - \ln(\delta) - \left(1+\frac{1}{\xi_t}\right)\ln\left(1+\xi_t\frac{x_t}{\delta}\right)\right] \\ &+ \mathrm{I}(x_t=0)\ln(1-(1+\tau)^{-\frac{1}{\xi_t}}).\end{aligned}$$

The derivation of the score follows Appendix A1, with some adjustments. In particular,

$$\begin{aligned}\nabla_t &= \frac{\partial\ell(x_t;\delta,\xi_t)}{\partial f_t} = \frac{\partial\ell(x_t;\delta,\xi_t)}{\partial\xi_t}\cdot\frac{\mathrm{d}\xi_t}{\mathrm{d}f_t}, \\ \frac{\partial\ell(x_t;\delta,\xi_t)}{\partial\xi_t} &= \mathrm{I}(x_t>0)\left[\frac{1}{\xi_t^2}\ln\left(1+\xi_t\frac{x_t}{\delta}\right) - \frac{\xi_t+1}{\xi_t}\frac{x_t}{\delta+\xi_t x_t}\right] \qquad \text{(A5)} \\ &+ \mathrm{I}(x_t>0)\left[\frac{1}{\xi_t^2}\ln(1+\tau)\right] + \mathrm{I}(x_t=0)\left[\frac{1}{\xi_t^2}\ln(1+\tau)\right] \qquad \text{(A6)} \\ &- \mathrm{I}(x_t=0)\left[\frac{1}{1-(1+\tau)^{-\frac{1}{\xi_t}}}\frac{1}{\xi_t^2}\ln(1+\tau)\right] \qquad \text{(A7)} \\ \frac{\mathrm{d}\xi_t}{\mathrm{d}f_t} &= \exp(f_t).\end{aligned}$$

The first part of the score (A5) is the same as in Appendix A1. (A5) is adjusted by (A6)–(A7) to take account of the point mass at zero. Combining (A5)–(A7) yields (9).

As before, the scaling function is the inverse conditional Fisher information of the mixture density,

$$\mathcal{S}_t = \mathrm{E}[\nabla_t^2|\mathcal{F}_{t-1};f_t,\psi]^{-1} = \mathrm{E}\left[-\frac{\partial^2\ell(x_t;\delta,\xi_t)}{\partial\xi_t^2}\right]^{-1}\exp(-2f_t).$$

The expectation of the negative second derivative is given by the sum of three expected negative

partial derivatives of (A5)–(A7). Specifically,

$$\begin{aligned}
\mathrm{E}\left[-\frac{\partial^2 \ell(x_t;\delta,\xi_t)}{\partial \xi_t^2}\right] &= \mathrm{E}\left[-\frac{\partial\ (\mathrm{A5})}{\partial \xi_t}\right] + \mathrm{E}\left[-\frac{\partial\ (\mathrm{A6})}{\partial \xi_t}\right] + \mathrm{E}\left[-\frac{\partial\ (\mathrm{A7})}{\partial \xi_t}\right], \\
\text{where} \quad \mathrm{E}\left[-\frac{\partial\ (\mathrm{A5})}{\partial \xi_t}\right] &= \frac{2(1+\tau)^{-\frac{1}{\xi_t}}}{(1+2\xi_t)(1+\xi_t)}, \qquad (\mathrm{A8}) \\
\mathrm{E}\left[-\frac{\partial\ (\mathrm{A6})}{\partial \xi_t}\right] &= \frac{2}{\xi_t^3}\ln(1+\tau), \qquad (\mathrm{A9}) \\
\mathrm{E}\left[-\frac{\partial\ (\mathrm{A7})}{\partial \xi_t}\right] &= \frac{(1+\tau)^{-\frac{1}{\xi_t}}}{1-(1+\tau)^{-\frac{1}{\xi_t}}}\frac{1}{\xi_t^4}\ln(1+\tau)^2 - \frac{2}{\xi_t^3}\ln(1+\tau), \qquad (\mathrm{A10})
\end{aligned}$$

and where (A8) follows from the result in Appendix A1. The indicator functions in (A5)–(A7) disappear as they determine the domain of integration when taking expectations. Note that (A10) does not require integration, but evaluation at a point mass. Combining terms, we obtain (10) in closed form as

$$\mathcal{S}_t = \left[\frac{2\xi_t^2(1+\tau)^{-\frac{1}{\xi_t}}}{(1+2\xi_t)(1+\xi_t)} + \frac{(1+\tau)^{-\frac{1}{\xi_t}}}{1-(1+\tau)^{-\frac{1}{\xi_t}}}\frac{1}{\xi_t^2}\ln(1+\tau)^2\right]^{-1}.$$

References

Adrian, T. and H. S. Shin (2010). Liquidity and leverage. *Journal of Financial Intermediation 19*(3), 418–437.

Allen, L., T. G. Bali, and Y. Tang (2012). Does systemic risk in the financial sector predict future economic downturns? *Review of Financial Studies 25*(10), 3000–3036.

Blasques, F., S. J. Koopman, and A. Lucas (2015). Information theoretic optimality of observation driven time series models for continuous responses. *Biometrika 102*(2), 325–343.

Brownlees, C. T. and R. Engle (2015). SRisk: A conditional capital shortfall index for systemic risk measurement. *Unpublished working paper*.

Chavez-Demoulin, V. and P. Embrechts (2010). Revisiting the edge, ten years on. *Communications in StatisticsTheory and Methods 39*(8-9), 1674–1688.

Chavez-Demoulin, V., P. Embrechts, and S. Sardy (2014). Extreme-quantile tracking for financial time series. *Journal of Econometrics 181*(1), 44–52.

Cœuré, B. (2013). Outright Monetary Transactions, one year on. Speech at the conference "The

ECB and its OMT programme," Berlin, 2 September 2013.

Cox, D. R. (1981). Statistical analysis of time series: some recent developments. *Scandinavian Journal of Statistics 8*, 93–115.

Creal, D., S. J. Koopman, and A. Lucas (2013). Generalized autoregressive score models with applications. *Journal of Applied Econometrics 28*(5), 777–795.

Creal, D., B. Schwaab, S. J. Koopman, and A. Lucas (2014). An observation driven mixed measurement dynamic factor model with application to credit risk. *The Review of Economics and Statistics 96(5)*, 898915.

Davidson, A. C. and R. L. Smith (1990). Models for exceedances over high thresholds. *Journal of the Royal Statistical Association, Series B 52*(3), 393–442.

ECB (2013). European Central Bank Annual Report 2012.

Embrechts, P., C. Klüppelberg, and T. Mikosch (1997). *Modelling extremal events for insurance and finance*. Springer Verlag, Berlin.

Eser, F., M. Carmona Amaro, S. Iacobelli, and M. Rubens (2012). The use of the Eurosystem's monetary policy instruments and operational framework since 2009. ECB Occasional Paper 135, European Central Bank.

Eser, F. and B. Schwaab (2016). Evaluating the impact of unconventional monetary policy measures: Empirical evidence from the ecb's securities markets programme. *Journal of Financial Economics 119*(1), 147–167.

Galbraith, J. W. and S. Zernov (2004). Circuit breakers and the tail index of equity returns. *Journal of Financial Econometrics 2*(1), 109–129.

Ghysels, E., J. Idier, S. Manganelli, and O. Vergote (2016). A high frequency assessment of the ECB Securities Markets Programme. *Journal of European Economic Association, forthcoming*.

González-Páramo, J.-M. (2011). The ECB's monetary policy during the crisis. Closing speech at the Tenth Economic Policy Conference, Málaga, 21 October 2011.

Hartmann, P., S. Straetmans, and C. de Vries (2004). Asset market linkages in crisis periods. *Review of Economics and Statistics 86(1)*, 313–326.

Hartmann, P., S. Straetmans, and C. de Vries (2007). Banking system stability: A cross-atlantic perspective. In M. Carey and R. M. Stulz (Eds.), *The Risks of Financial Institutions*, pp. 1–61. NBER and University of Chicago Press.

Harvey, A. C. (2013). *Dynamic models for volatility and heavy tails: with applications to financial and economic time series*. Number 52. Cambridge University Press.

Kelly, B. (2014). The dynamic power law model. *Extremes 17*(4), 557–583.

Kelly, B. and H. Jiang (2014). Tail risk and asset prices. *Review of Financial Studies*, 2841–2871.

Lewis, J. B. and D. A. Linzer (2005). Estimating regression models in which the dependent variable is based on estimates. *Political Analysis 13*, 345364.

Lucas, A., B. Schwaab, and X. Zhang (2014). Conditional euro area sovereign default risk. *Journal of Business and Economics Statistics 32*(2), 271–284.

Lucas, A., B. Schwaab, and X. Zhang (2016). Modeling financial sector joint tail risk in the euro area. *Journal of Applied Econometrics, forthcoming*.

Lucas, A. and X. Zhang (2016). Score driven exponentially weighted moving averages and Value-at-Risk forecasting. *International Journal of Forecasting, forthcoming*.

Massacci, D. (2014). Tail risk dynamics in stock returns: links to the macroeconomy and global markets connectedness. Technical report.

McNeil, A. and R. Frey (2000). Estimation of tail-related risk measures for heteroscedastic financial time series: An extreme value approach. *Journal of Empirical Finance 7*(3-4), 271–300.

McNeil, A. J., R. Frey, and P. Embrechts (2010). *Quantitative risk management: Concepts, techniques, and tools*. Princeton University press.

Pagan, A. (1984). Econometric issues in the analysis of regressions with generated regressors. *International Economic Review 25(1)*, 221247.

Pelizzon, L., M. Subrahmanyam, D. Tomio, and J. Uno (2013). The microstructure of the European sovereign bond market: A study of the Eurozone crisis. Unpublished working paper, University of Venice, New York University, Copenhagen Business School, and Waseda University.

Poon, S., M. Rockinger, and J. Tawn (2004). Extreme value dependence in financial markets. *Review of Financial Studies 17(2)*, 581–610.

Quintos, C., Z. Fan, and P. C. Phillips (2001). Structural change tests in tail behaviour and the asian crisis. *The Review of Economic Studies 68*(3), 633–663.

Rocco, M. (2014). Extreme value theory in finance: A survey. *Journal of Economic Surveys 28*(1), 82–108.

Vayanos, D. and J.-L. Vila (2009). A preferred habitat model of the term structure of interest rates. NBER Working Paper 15487.

Wagner, N. (2005). Autoregressive conditional tail behavior and results on government bond yield spreads. *International Review of Financial Analysis 14*(2), 247–261.

Werner, T. and C. Upper (2004). Time variation in the tail behavior of bund future returns. *Journal of Futures Markets 24*(4), 387–398.